Matrix Effect on Hydrogen Atom Tunneling: Comparison between Hydrogen Addition and Abstraction

Tsuneki Ichikawa,* Takeshi Takahashi, Hitoshi Koizumi, and Tomoya Takada

Division of Molecular Chemistry, Graduate School of Engineering, Hokkaido University, Sapporo, 060-8628 Japan

Received: October 12, 1999

Hydrogen-atom tunneling from and to linear alkenes in organic matrices at 77 K has been studied for elucidating the effect of matrices on the rate of the tunneling. The rate of hydrogen-atom addition to the vinyl carbon of alkenes does not depend on the length of alkyl chains bonded to the vinyl carbon, whereas the rate of hydrogen-atom abstraction by methyl radicals from the allylic carbon decreases with increasing length of alkyl chains bonded to the allylic carbon. These effects are explained as due to the resistance of matrices to the change of the C−C−C bond angle of the reacting carbon during the tunneling. For hydrogen-atom abstraction, the resistance causes the increase of the height of the potential barrier between the entrance and the exit of the tunneling channel, whereas the resistance does not cause the retardation of the tunneling to the vinyl carbon since the bond angle scarcely changes during the tunneling.

Introduction

Although the tunneling of atoms through potential energy barriers separating reactant and product systems is not paid much attention in organic reactions, this plays an important role in reactions including the transfer of light atoms. Atomic tunneling is especially important for chemical reactions at low temperatures, since the thermal activation of reactant systems is a very slow process in comparison with the tunneling.

One of the typical reactions of atomic tunneling is hydrogen-atom abstraction from alkanes in cryogenic solids exposed to high-energy radiation. Irradiation of alkane molecules causes the homolytic cleavage of C−H bonds, which results in pairwise formation of free hydrogen atoms and organic free radicals. Since the activation energies for the abstraction of hydrogen atoms from alkane molecules by free hydrogen atoms are higher than 5 kcal/mol, the lifetime of free hydrogen atoms at 77 K is estimated from the Arrhenius equation to be longer than 10 h. However, except for solid methane, free hydrogen atoms immediately convert to alkyl radicals even at 4.2 K by hydrogen-atom tunneling from alkane molecules to the free hydrogen atoms.[1]

The rate of hydrogen atom tunneling does not necessarily increase with the decrease of the activation energy or the peak height of the potential energy barrier separating a reactant and a product system. Although the activation energy and the bond dissociation energy is the lowest at the tertiary carbon of alkanes, Henderson and Willard found a very strange reaction that the rupture of C−H bonds by the attack of hydrogen atoms or by γ-ray and UV irradiation selectively took place in rigid cryogenic matrices at the antepenultimate secondary carbon of branched alkanes with tertiary carbon at the antepenultimate position.[2] Ichikawa and Ohta then showed that the location of the selective rupture could be changed to the tertiary C−H bond by replacing the $-CH_2CH_3$ group with $-CD_2CH_3$.[3,4] Using ESR and electron spin echo spectroscopy, we found that the selective C−H bond rupture at the penultimate secondary carbon was due to the conversion of primary alkyl radicals and free hydrogen atoms to penultimate secondary alkyl radicals by selective hydrogen-atom tunneling from the penultimate position of the carbon skeleton.[5,6] On the basis of the observation that the preferential position of hydrogen-atom tunneling from the branched alkane changed to the antepenultimate tertiary carbon by changing the matrix to crystalline adamantane, in which the branched alkane could move rather freely even at 77 K, we proposed that the peculiarity of the hydrogen abstraction in cryogenic solids arose from the resistance of matrix molecules to the deformation of alkane molecules from the initial sp^3 to the final sp^2 configuration.[7] The resistance increases with the increasing number and length of alkyl chains bonded to a carbon atom to be hydrogen-abstracted. Increase of the resistance causes the increase of the area of the potential energy barrier for the tunneling. Since the rate of the tunneling depends exponentially on the area of the barrier, the penultimate secondary carbon shows the highest tunneling rate in rigid matrices; even the peak height of the barrier is higher than that for the antepenultimate tertiary carbon.

To study the detail of the matrix effect on hydrogen-atom tunneling is interesting not only from the theoretical point of view but also from the practical point of view. The area of a tunneling barrier is sensitive to the rigidity of a matrix, which suggests a new possibility of the mechanical control of the rate of chemical reactions by changing the viscosity of a solvent. In the present study, the relative rates of hydrogen-atom tunneling to one of two vinyl carbon atoms of linear alkenes and from one of two allylic carbon atoms to the methyl radicals at 77 K have been measured for elucidating the general feature of matrix effects on the tunneling rate. The reactions of free hydrogen atoms in cryogenic solids with alkenes have been studied by several researchers.[8−10] It is established from these studies that the principal primary process is hydrogen-atom tunneling to the less substituted vinyl carbon.[8] However it is not clear whether the rate of tunneling depends on the length of the substituted alkyl groups.

10.1021/jp9936291 CCC: $19.00
Published on Web 03/07/2000

Experimental Section

Linear alkenes used were 1-hexene, *trans*-2-hexene, and *trans*-3-hexene. Partially deuterated methanol, CD_3OH, was used as a matrix for studying hydrogen-atom addition to solute alkenes. The concentration of alkenes was 2 vol %. Free hydrogen atoms were generated at 77 K by photoionization of triphenylamine in the methanol matrices followed by the attachment of photoejected electrons to protons, as

$$(C_6H_5)_3N + 2h\nu \rightarrow (C_6H_5)_3N^+ + e^-$$

$$e^- + HCl \rightarrow H + Cl^-$$

The concentrations of $(C_6H_5)_3N$ and HCl were about 10 mmol/dm^3 and 0.1 mol/dm^3, respectively. The ESR spectra of alkyl radicals generated by the hydrogen-atom addition were compared with those generated by the attachment of the photoejected electrons to chlorinated alkanes in CD_3OD matrices,[5] as

$$e^- + R^1R^2R^3CCl \rightarrow R^1R^2R^3C + Cl^-$$

The concentration of the chlorinated alkanes was about 2 vol %. Methyl radicals were generated at 77 K by photoionization of $(C_6H_5)_3N$ in the alkene matrices followed by the dissociative electron attachment to CH_3Br. The concentrations of $(C_6H_5)_3N$ and CH_3Br in the alkenes were about 10 mmol/dm^3 and 0.1 mol/dm^3, respectively. The samples were degassed before irradiation by repeated freezing−pumping−warming cycles. The photoionizations were carried out with UV light of $\lambda > 300$ nm from a Xe arc lamp. Irradiation with UV light of $\lambda < 300$ nm caused the photoconversion of product radicals.[11,12] The X-band ESR spectra of free radicals generated by the irradiation were recorded at 77 K. Quantum-chemical calculations of potential energy barriers for the formation of free radicals from the alkenes were made by using the MP2/3-21G program in the Gaussian 98 software. Comparison of the calculations for a propene + H system with MP2/3-21G and more accurate but time-consuming MP2/6-31G** showed that the barrier heights and the structures of the transition states were scarcely changed by the basis sets.

Results and Discussion

Hydrogen-Atom Addition to Vinyl Carbon. The ESR spectra of irradiated alkene/methanol samples were composed of a narrow intense spectrum due to solvent radicals and wider ones due to solute alkyl radicals. The yield of alkyl radicals was more than 50% of the total radical yield, which indicates that the addition of free hydrogen atoms to the vinyl carbon of solute alkanes is much faster than the abstraction of deuterium atoms from methanol. No hydrogen atom was observed during the irradiation, which implies that the hydrogen atoms react with solute and solvent molecules immediately after the formation. Since the concentration of alkenes was only 2 vol %, it is reasonable to assume that hot hydrogen atoms generated by the reaction of photoejected electrons with HCl were thermalized before encountering alkene molecules by colliding with many matrix molecules.[13] Figure 1 compares the ESR spectrum of alkyl radicals generated from $CH_2{=}CH(CH_2)_3CH_3$ with those of $CH_3C^*H(CH_2)_3CH_3$ and $C^*H_2(CH_2)_4CH_3$ generated from the corresponding chlorohexane by the dissociative electron attachment. Here C* denotes the radical carbon. The ESR spectrum is close to that of $CH_3C^*H(CH_2)CH_3$, which confirms the conclusion of previous studies that hydrogen atoms preferentially tunnel to the less substituted carbon of the double bond of alkenes.[8]

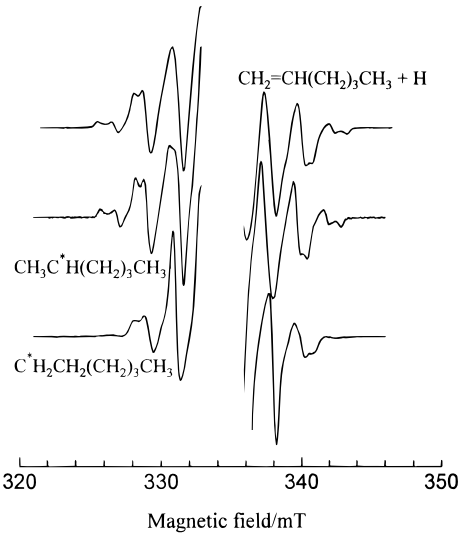

Figure 1. Comparison of the ESR spectrum of alkyl radicals generated by the addition of H atoms to $CH_2{=}CH(CH_2)_3CH_3$ in CD_3OH matrix at 77 K with those of $CH_3C^*H(CH_2)_3CH_3$ and $C^*H_2CH_2(CH_2)_3CH_3$ radicals.

The selective addition of hydrogen atoms to the terminal vinyl carbon is simply due to the lower barrier for hydrogen-atom tunneling. The tunneling rate of a particle with reduced mass μ is expressed by

$$k \approx \exp\{-2^{3/2}\hbar \int_a^b \sqrt{\mu[U(r) - E_r]}\, dr\} \qquad (1)$$

Here $U(r)$ is a potential energy barrier separating an initial reactant state and a final product state, E_r is the energy of the reactant state, and a and b are the locations of the entrance and the exit of a tunneling channel where the potential energies are equal to E_r. The rate of tunneling depends exponentially on the square root of the area of the potential energy barrier above the initial energy and considerably decreases with increasing height and width of the barrier. As shown in Table 1, the peak height of the barrier or the activation energy for hydrogen-atom addition to the terminal vinyl carbon is about 1 kcal/mol lower than that to the penultimate one, which is low enough for the selective addition of hydrogen atoms to the terminal carbon.

Figure 2 compares the ESR spectra of free radicals generated from $CH_3CH_2CH{=}CHCH_2CH_3$ with that of $CH_3CH_2C^*H(CH_2)_2CH_3$ generated by the dissociative electron attachment. Since $CH_3CH_2CH{=}CHCH_2CH_3$ is symmetric with respect to the double bond, the radical generated is undoubtedly $CH_3CH_2C^*H(CH_2)_2CH_3$. A small difference between the two spectra arises from the difference of the amount the solvent radicals.

Two kinds of alkyl radicals, $CH_3C^*HCH_2(CH_2)_2CH_3$ and $CH_3CH_2CH^*(CH_2)_2CH_3$, are possibly generated by hydrogen-atom addition to 2-hexene, $CH_3CH{=}CH(CH_2)_2CH_3$. As shown in Figure 3, the ESR spectrum of free radicals generated from $CH_3CH{=}CH(CH_2)_2CH_3$ can be reproduced as the 1:1 mixture of $CH_3C^*H(CH_2)CH_3$ and $CH_3CH_2CH^*(CH_2)_2CH_3$ generated from $CH_2{=}CH(CH_2)_3CH_3$ and $CH_3CH_2CH{=}CHCH_2CH_3$, respectively. The reactivity of the vinyl carbon toward hydrogen-atom addition is therefore independent of the chain length of the substituted alkyl group.

We have shown in the previous paper[7] that the rate of hydrogen-atom tunneling from hexane to hydrogen atoms in cryogenic glassy matrices decreases with the increasing length of alkyl chains attached to reacting carbon atoms, because the increases of the length causes the increase of steric hindrance

TABLE 1: Observed Yields and Peak Heights of Potential Energy Barriers for the Formation of Free Radicals from Linear Alkenes

reactant	product	rel yield	peak height, kcal/mol[a] (activation energy)	
$CH_2{=}CH(CH_2)_3CH_3 + H$	$CH_3C^*H(CH_2)_3CH_3$	1	3.2 (1.5[b])	
	$C^*H_2CH_2(CH_2)_3CH_3$	0	4.6 (2.8[b])	
$CH_3CH{=}CH(CH_2)_2CH_3 + H$	$CH_3CH_2C^*H(CH_2)_2CH_3$	1	4.7	(2.1[b])
	$CH_3C^*HCH_2(CH_2)_2CH_3$	1	4.6	
$CH_2{=}CH(CH_2)_3CH_3 + CH_3$	$CH_3CH_2C^*H(CH_2)_3CH_3$	1	6.5 (7.4?[c])	
	$C^*H_2C^*HC^*H(CH_2)_2CH_3 + CH_4$	5	11.5, 35.8[d] (7.4? + 1.9[c])	
$CH_3CH{=}CH(CH_2)_2CH_3 + CH_3$	$C^*H_2C^*HC^*H(CH_2)_2CH_3 + CH_4$	4	12.6, 36.8[d] (7.4? + 3.4[c])	
	$CH_3C^*HC^*HC^*HC_2H_5 + CH_4$	1	11.2, 35.8[d] (7.4? + 1.9[c])	

[a] MP2/3-21G ab initio calculation. [b] Experimental value cited from ref 17. [c] Experimental value cited from ref 15. Marked with ? is an inaccurate value. [d] Calculated value under the fixed C(methyl)−C(allyl) distance of 3.6×10^{-8} cm.

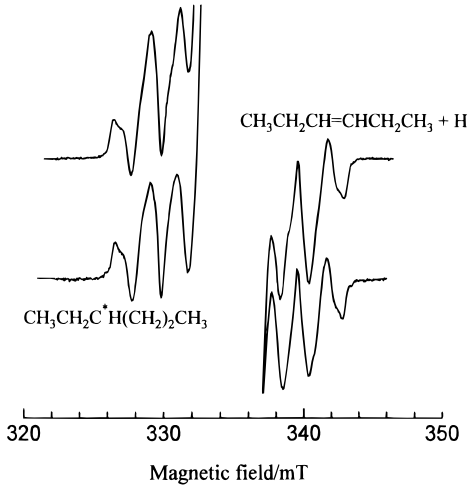

Figure 2. Comparison of the ESR spectrum of alkyl radicals generated by the addition of H atoms to $CH_3CH_2CH{=}CHCH_2CH_3$ in CD_3OH matrix at 77 K with that of $CH_3CH_2C^*H(CH_2)_2CH_3$ radicals.

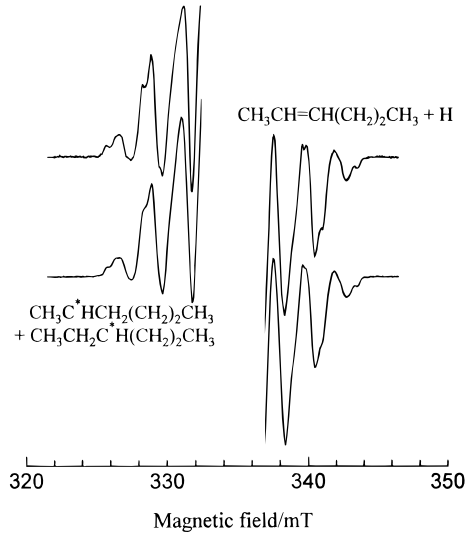

Figure 3. Comparison of the ESR spectra of alkyl radicals generated by the addition of H atoms to $CH_3CH{=}CH(CH_2)_2CH_3$ in CD_3OH matrix at 77 K with that of simulated one obtained by assuming the presence of the same amount of $CH_3C^*HCH_2(CH_2)_2CH_3$ and $CH_3CH_2C^*H(CH_2)_2CH_3$ radicals.

by matrix molecules to the deformation of hexane from the initial sp^3 to the final sp^2 configuration and thereby causes the increase of the area of the tunneling barrier. If this explanation were applicable to the hydrogen-atom addition, the addition to the penultimate vinyl carbon of $CH_3CH{=}CH(CH_2)_2CH_3$ would be faster than that to the antepenultimate one. However, the rates were the same.

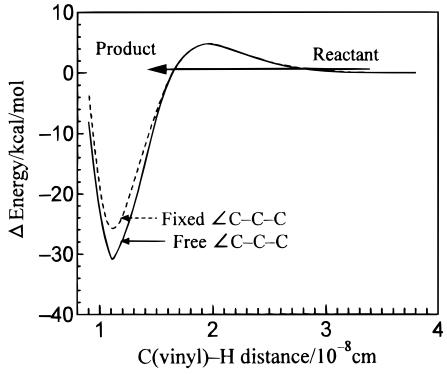

Figure 4. Potential energy surfaces for $CH_3CH{=}CH(CH_2)_2CH_3 + H \rightarrow CH_3CH_2C^*H(CH_2)_2CH_3$ under the reaction conditions of free C−C−C bending motion for 2-hexene and of the fixed C−C−C bond angles at the initial 2-hexene.

This discrepancy can be explained by taking the difference of the structural changes of the reaction systems during the tunneling processes into consideration. Hydrogen-atom abstraction from alkanes results in the change of the bond orbitals of the reacting carbon from the initial sp^3 to the final sp^2 configuration, which accompanies the change of the C−C−C bond angle. As shown in the previous paper,[7] the optimized geometrical structure of the reaction system at the exit of the tunneling channel is not far from the product state, so that the suppression of the angular change by matrix molecules causes the increase of the potential energy and thereby a decrease of the tunneling rate. The suppression is larger for longer alkyl chains, so that hydrogen atoms are preferentially abstracted from carbon atoms with shorter alkyl chains, even if the rate of hydrogen-atom abstraction by thermal activation is the same or slower. Hydrogen-atom addition to alkenes results in the change of the bond orbitals of the vinyl carbon from the initial sp^2 to the final sp^3 configuration, which also accompanies the change of the C−C−C bond angle. However, the effect of matrix molecules on the tunneling is not the same. Figure 4 shows the shape of the potential energy barriers for hydrogen-atom addition to the penultimate vinyl carbon of $CH_3CH{=}CH(CH_2)_2CH_3$ as calculated with MP2/3-21G under two different reaction conditions: no restriction on the motion of atoms (optimized barrier) and the fixed C−C−C bond angles of initial $CH_3CH{=}CH(CH_2)_2CH_3$. The first and the second conditions simulate the hydrogen-atom tunneling in a vacuum and in a rigid matrix in which the change of the C−C−C bond angles is highly restricted, respectively. Contrary to hydrogen-atom abstraction from alkanes, the shape of the barrier above the tunneling channel is scarcely changed by the restriction posed to $CH_3CH{=}CH(CH_2)_2CH_3$. This implies that the change of the bond angles is not necessary even at the exit of the optimum

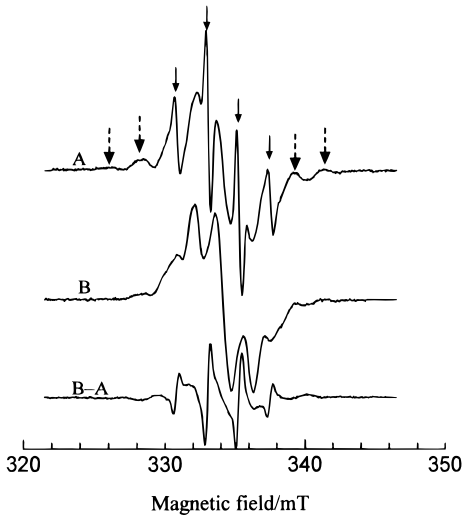

Figure 5. ESR spectra of free radicals observed (A) immediately and (B) 10 h after the formation of C^*H_3 in solid $CH_2{=}CH(CH_2)_3CH_3$ at 77 K. Solid and broken arrows indicate the hyperfine lines of C^*H_3 and $CH_3CH_2C^*H(CH_2)_3CH_3$ radicals. The difference spectrum of A and B is also shown.

tunneling channel. Since the suppression of the angular change scarcely affects the rates of hydrogen-atom addition, the tunneling rate is independent of the length of the alkyl group substituted to the vinyl carbon, as long as the shape of the optimized potential energy barrier above the tunneling channel does not depend on the length of the substituted alkyl group. As shown in Table 1, the calculated shape of the optimized potential energy barrier scarcely depends on the length of the substituted alkyl group.

Our present result is in marked contrast with that obtained by Bennet et al.[9] On the basis of the analysis of their ESR spectra, they concluded that hydrogen-atom addition in an adamantane matrix at 77 K to the penultimate vinyl carbon of $CH_3CH{=}CHCH_2CH_3$ was more than 7 times faster than that to the antepenultimate one. Although we do not know the reason for the discrepancy, it may be worthwhile to point out that the spectral separation of the resultant $CH_3C^*HCH_2CH_2CH_3$ and $CH_3CH_2C^*HCH_2CH_3$ radicals is very difficult, since both of them give octet spectra with the separation of 2.2 mT.[7] Our result is in agreement with that by Kelley et al.[8] On the basis of product analyses, they concluded that the tunneling rate of hydrogen atoms to the penultimate vinyl carbon of $CH_3CH{=}CHCH_2CH_3$ was the same as that to the antepenultimate one.

Hydrogen-Atom Abstraction by Methyl Radicals. Figure 5 shows the spectral change for $CH_2{=}CH(CH_2)_3CH_3$ at 77 K after UV irradiation. The ESR spectrum at 5 min after the irradiation (spectrum A) is composed of three components: a sharp quartet with the separation of 2.3 mT (solid arrows), a broad octet with the separation of 2.2 mT (broken arrows), and a broad septet with the separation of 1.45 mT. The sharp quartet is obviously due to C^*H_3. The broad octet is due to alkyl radicals, probably $CH_3CH_2C^*H(CH_2)_3CH_3$, generated by the addition of C^*H_3 to the terminal vinyl carbon. The broad septet is attributable to $C^*H_2C^*HC^*H(CH_2)_2CH_3$, since the spectrum accords well with that of allyl-type $C^*H_2C^*HC^*HCH_2-$ radicals generated by γ-irradiation of 1-alkenes.[14] The ESR spectrum of $(C_6H_5)_3N^+$ is not detectable due probably to too broad hyperfine lines arising from ^{14}N. Analysis of spectrum A shows that the concentration of $C^*H_2C^*HC^*H(CH_2)_2CH_3$ is more than 5 times of that of the alkyl radicals. The concentrations of C^*H_3 and the alkyl radicals gradually decrease with time. Although

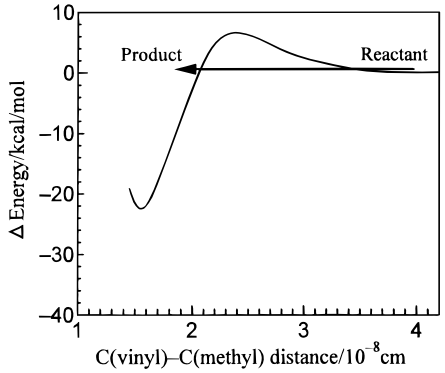

Figure 6. Potential energy surface for $CH_2{=}CH(CH_2)_3CH_3 + C^*H_3 \rightarrow CH_3CH_2C^*H(CH_2)_3CH_3$.

C^*H_3 completely disappears at 10 h after the irradiation (spectrum B), the total concentration of radical species is kept constant. Subtraction of spectrum B from spectrum A gives spectrum C that is composed of negative spectra of C^*H_3 and the alkyl radicals and the positive spectrum of $C^*H_2C^*HC^*H(CH_2)_2CH_3$. This is direct evidence of the gradual conversion of C^*H_3 and the alkyl radicals to $C^*H_2C^*HC^*H(CH_2)_2CH_3$ by hydrogen-atom abstraction from the allylic carbon of $CH_2{=}CH(CH_2)_3CH_3$. Hydrogen-atom abstraction by the alkyl radicals is much slower than that by C^*H_3, since the alkyl radicals still remain at 10 h after the formation.

The ESR results on $CH_3CH_2CH{=}CHCH_2CH_3$ are essentially the same as those on $CH_2{=}CH(CH_2)_3CH_3$. Although a small amount of $CH_3CH_2CH(CH_3)C^*HCH_2CH_3$ is generated, the major reaction of C^*H_3 with $CH_3CH_2CH{=}CHCH_2CH_3$ is the formation of $CH_3C^*HC^*H{-}C^*HCH_2CH_3$ by hydrogen-atom abstraction from the allylic carbon.

The alkyl and allyl-type radicals are probably generated by the reaction of alkenes with hot and cold C^*H_3, respectively, as

$$CH_3Br + e^- \rightarrow C^*H_3\ (\text{hot}) + Br^-$$

$$C^*H_3\ (\text{hot}) + \text{alkene} \rightarrow \text{alkyl radical}$$

$$C^*H_3\ (\text{hot}) \rightarrow C^*H_3\ (\text{cold})$$

$$C^*H_3\ (\text{cold}) + \text{alkene} \rightarrow \text{allyl-type radical}$$

Because of lower activation energy, the major thermal reaction of C^*H_3 with alkenes is not the abstraction of hydrogen atoms from the allylic carbon but the addition of C^*H_3 to the vinyl carbon.[15] The addition at room temperature is 8 times faster than the abstraction. The change of the major reaction at 77 K from the addition to the abstraction indicates that the abstraction takes place through the tunneling of hydrogen atoms. As shown in Figure 6, the addition of C^*H_3 to the vinyl carbon necessitates the tunneling of more than 1.3×10^{-8} cm. Since the effective distance of tunneling is a product of a tunneling distance and the square-root mass of a tunneling particle, the tunneling of heavy C^*H_3 is much slower than that of hydrogen atoms even though the tunneling barrier is lower.

Two kinds of allyl-type radicals, $C^*H_2C^*HC^*H(CH_2)_2CH_3$ and $CH_3C^*HC^*HC^*HCH_2CH_3$, are expected to be generated from $CH_3CH{=}CH(CH_2)_2CH_3$ by hydrogen-atom abstraction. As shown in Figure 7, the ESR spectrum of free radicals generated from $CH_3CH{=}CH(CH_2)_2CH_3$ can be reproduced as the 4:1 mixture of $C^*H_2C^*HC^*H(CH_2)_2CH_3$ and $CH_3C^*HC^*HC^*HCH_2CH_3$, which suggests that hydrogen-atom abstraction from the allylic carbon with a shorter alkyl chain is 4 times faster than that with a longer one.

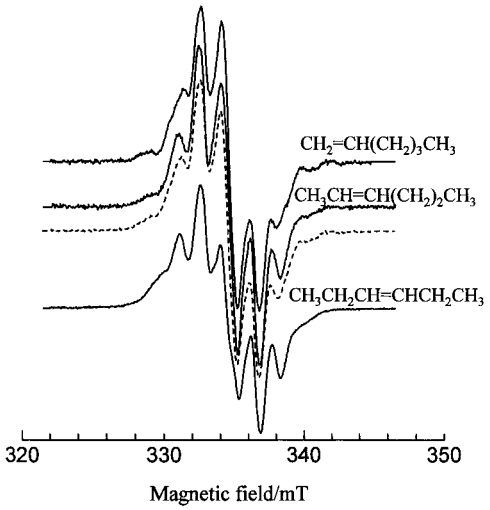

Figure 7. Comparison of the ESR spectra of allyl-type radicals generated from $CH_2{=}CH(CH_2)_3CH_3$, $CH_3CH{=}CH(CH_2)_2CH_3$, and $CH_3CH_2CH{=}CHCH_2CH_3$ by hydrogen-atom abstraction at 77 K. The spectrum for $CH_3CH{=}CH(CH_2)_2CH_3$ can be simulated as the 4:1 mixture of $C^*H_2C^*HC^*H(CH_2)_2CH_3$ and $CH_3C^*HC^*HC^*HCH_2CH_3$ radicals (- - -).

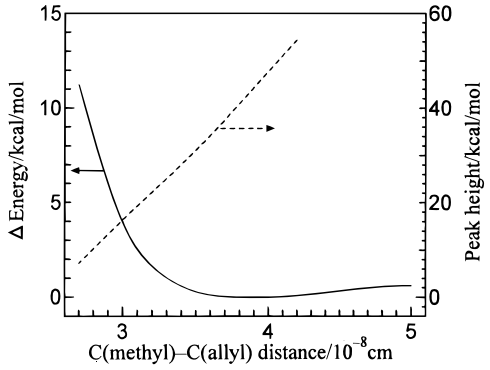

Figure 8. Potential energy barrier for the approach of C^*H_3 toward the allylic carbon of $CH_3CH{=}CH(CH_2)_2CH_3$. The peak height of the potential energy barrier for hydrogen-atom transfer from the allylic carbon to C^*H_3 at each C(methyl)−C(allyl) distance is also given with a broken line.

Hydrogen-atom abstraction at room temperature from the allylic carbon of 2-alkene is known to be 10 times faster than that from the terminal allylic carbon,[16] since the activation energy is lower for the former one. However, the abstraction from the terminal allylic carbon is 4 times faster at 77 K. The reversal of the selectivity of hydrogen-atom abstraction can be understood by taking the structural change of the reaction system during the tunneling into consideration. The tunneling of a hydrogen atom is the fastest at the C (methyl)−H−C(allyl) collinear structure. Figure 8 shows the energy for making the collinear structure as a function of the C(methyl)−C(allyl) distance. The peak height of the potential energy barrier for the tunneling at a given C(methyl)−C(allyl) distance is also shown. The optimum transition state is attained at the C(methyl)−C(allyl) distance of 2.7×10^{-8} cm. However, it is impossible for the reaction system at 77 K to pass the optimum transition state, because more than 10 kcal/mol of thermal energy is necessary for attaining this configuration. Since the collinear structure is stable at the distance of $(3.6-4) \times 10^{-8}$ cm, it is reasonable to assume that the tunneling of the hydrogen atom takes place at the C(methyl)−C(allyl) distance of 3.6×10^{-8} cm.

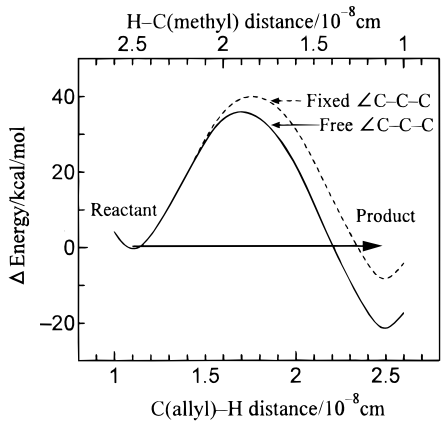

Figure 9. Potential energy surfaces for $C^*H_3 + CH_2{=}CH(CH_2)_3CH_3 \rightarrow CH_4 + C^*H_2C^*HC^*H(CH_2)_2CH_3$ under the reaction conditions of free C−C−C bending motion for 1-hexene and of the fixed C−C−C bond angles at the initial 1-hexene.

Figure 9 shows the shapes of potential energy barriers for hydrogen-atom abstraction from the antepenultimate allylic carbon of $CH_2{=}CH(CH_2)_3CH_3$ at the fixed C(methyl)−C(allyl) distance of 3.6×10^{-8} cm as calculated with MP2/3-21G under two different reaction conditions: no restriction on the motion of atoms except for the tunneling atom (optimized barrier) and the fixed C−C−C bond angles of initial $CH_2{=}CH(CH_2)_3CH_3$. The first and the second conditions simulate the hydrogen-atom tunneling in a vacuum and in a rigid matrix in which the change of the C−C−C bond angles is highly restricted, respectively. Contrary to hydrogen-atom addition to the vinyl carbon, the restriction of the angular change significantly increases the height of the barrier above the tunneling path. This is because the structures of the alkene at the transition state and at the exit of the tunneling channel are close to that of the product state. The location of the hydrogen atom at the transition state is far from the allylic carbon, so that the optimum C−C−C bond angle of the allylic carbon is close to the sp^2 angle of 120°. Restriction of the C−C−C bending motion toward the product system therefore causes a significant increase of the potential energy barrier. The restriction is more severe for the allylic carbon with a longer alkyl chain, so that the rate of hydrogen-atom abstraction is slower for the antepenultimate allylic carbon even though the optimum peak height of the tunneling barrier is lower.

Conclusion

It is generally concluded that the resistance of matrix molecules to the deformation of a reaction system from the initial reactant state to the final product state suppresses the tunneling of hydrogen atoms, if the configurations of atoms other than the tunneling particle are not the same at the entrance and the exit of the optimum tunneling channel. The effect of matrix on hydrogen-atom tunneling from and to alkene molecules in cryogenic solids is summarized as follows;

(1) Matrix molecules retard the abstraction of hydrogen atoms by methyl radicals from the allylic carbon of linear alkenes by restricting the C−C−C bending motion of the allylic carbon, which is necessary for changing the bond orbitals from sp^3 to sp^2 configuration. An increase of the length of alkyl chains bonded to the allyic carbon causes the increase of the resistance, which results in the retardation of the abstraction.

(2) Hydrogen-atom tunneling to the vinyl carbon of linear alkenes does not depend on the number and the length of alkyl chains bonded to the vinyl carbon, since the vinyl carbon does

not necessitate the change of the C−C−C bond angle during the tunneling.

Acknowledgment. This work was supported by a Grant-in Aid for Scientific Research from the Ministry of Education, Science, and Culture, Japan.

References and Notes

(1) Iwasaki, M.; Toriyama, K.; Muto, H.; Nunome, K.; Fukaya, M. *J. Phys. Chem*. **1980**, *85*, 1326 and references therein.
(2) Henderson, D. J.; Willard, J. E. *J. Am. Chem. Soc*. **1969**, *91*, 3014.
(3) Ichikawa, T.; Ohta, N. *J. Phys. Chem*. **1977**, *81*, 560.
(4) Ichikawa, T.; Ohta, N. *Radiat. Phys. Chem*. **1987**, *29*, 429.
(5) Ichikawa, T.; Yoshida, H. *J. Phys. Chem.* **1992**, *96*, 7661.
(6) Ichikawa, T.; Yoshida, H. *J. Phys. Chem.* **1992**, *96*, 7665.
(7) Ichikawa, T.; Kagei, K.; Tachikawa, H.; Ishitani, Y. *J. Phys. Chem. A* **1999**, *103*, 6288.
(8) Kelley, R. D.; Klein, R.; Scheer, M. D. *J. Phys. Chem.* **1970**, *74*, 4301 and references therein.
(9) Bennett, J. E.; Mile, B. *J. Chem. Soc., Faraday Trans. 1* **1973**, *69*, 1398.
(10) Hiraoka, K.; Matsunaga, K.; Shoda, T.; Takimoto, H. *Chem. Phys. Lett.* **1992**, *11*, 292.
(11) Koizumi, H.; Hosugi. S.; Yoshida, H. *J. Phys. Chem*. **1994**, *98*, 11089; **1996**, *100*, 4848.
(12) Takada, T.; Koizumi, H.; Kagei, K.; Ichikawa, T.; Yoshida, H. *J. Phys. Chem. A* **1997**, *101*, 4379.
(13) Toriyama, K.; Okazaki, M.; Matsuura, K. *Radiat. Phys. Chem*. **1991**, *37*, 15, and references therein.
(14) Roginskii, V. A.; Pshezhetskii, S. Ya. *Khim. Vysokikh Energii* **1970**, *4*, 240.
(15) Ingold, K. U. In *Free Radicals*; Koch, J. K., Ed.; Sohn Wiley & Sons: New York, 1973; Vol. 1, Chapter 2.
(16) Buckley, R. P.; Szwarc, M. *Proc. R. Soc. (London)* **1957**, *A240*, 396.
(17) Miyazaki, M. In *CRC Handbook of Radiation Chemistry*; Tabata, Y., Ito, Y., Tagawa, S., Eds.; CRC Press: Boca Raton, FL 1991; Chapter X, p C.2.